Open Access Full Text Article

ORIGINAL RESEARCH

High molecular weight chitosan derivative polymeric micelles encapsulating superparamagnetic iron oxide for tumor-targeted magnetic resonance imaging

Yunbin Xiao[1,*]
Zuan Tao Lin[2,*]
Yanmei Chen[1]
He Wang[1]
Ya Li Deng[2]
D Elizabeth Le[3]
Jianguo Bin[1]
Meiyu Li[1]
Yulin Liao[1]
Yili Liu[1]
Gangbiao Jiang[2]
Jianping Bin[1]

[1]State Key Laboratory of Organ Failure Research, Division of Cardiology, Nanfang Hospital, Southern Medical University, Guangzhou, People's Republic of China; [2]Department of Pharmaceutical Engineering, South China Agricultural University, Guangzhou, People's Republic of China; [3]Cardiovascular Division, Oregon Health and Science University, Portland, OR, USA

*These authors contributed equally to this work

Correspondence: Jianping Bin
Department of Cardiology, Nanfang Hospital, Southern Medical University, 1838 North Guangzhou Avenue, Guangzhou 510515, People's Republic of China
Tel +86 186 8048 8488
Fax +86 20 8771 2332
Email jianpingbin@126.com

Gangbiao Jiang
Department of Pharmaceutical Engineering, South China Agricultural University, 348 Wushan, Guangzhou 510642, People's Republic of China
Tel +86 20 8528 0293
Fax +86 20 8528 0292
Email jgb3h@163.com

Abstract: Magnetic resonance imaging (MRI) contrast agents based on chitosan derivatives have great potential for diagnosing diseases. However, stable tumor-targeted MRI contrast agents using micelles prepared from high molecular weight chitosan derivatives are seldom reported. In this study, we developed a novel tumor-targeted MRI vehicle via superparamagnetic iron oxide nanoparticles (SPIONs) encapsulated in self-aggregating polymeric folate-conjugated N-palmitoyl chitosan (FAPLCS) micelles. The tumor-targeting ability of FAPLCS/SPIONs was demonstrated in vitro and in vivo. The results of dynamic light scattering experiments showed that the micelles had a relatively narrow size distribution (136.60±3.90 nm) and excellent stability. FAPLCS/SPIONs showed low cytotoxicity and excellent biocompatibility in cellular toxicity tests. Both in vitro and in vivo studies demonstrated that FAPLCS/SPIONs bound specifically to folate receptor-positive HeLa cells, and that FAPLCS/SPIONs accumulated predominantly in established HeLa-derived tumors in mice. The signal intensities of T_2-weighted images in established HeLa-derived tumors were reduced dramatically after intravenous micelle administration. Our study indicates that FAPLCS/SPION micelles can potentially serve as safe and effective MRI contrast agents for detecting tumors that overexpress folate receptors.

Keywords: superparamagnetic iron oxide, magnetic resonance imaging, polymeric micelles, folate receptors, tumor-targeted MRI, N-palmitoyl chitosan

Introduction

In recent decades, several studies have identified novel tumor-targeted magnetic resonance imaging (MRI) contrast agents with great potential for cancer diagnosis.[1–8] Superparamagnetic iron oxide nanoparticles (SPIONs) are generally encapsulated by or conjugated with synthetic polymeric coatings, such as polyethylene glycol or polyether-imide, which are modified with targeting ligands to obtain tumor-targeted MRI contrast agents.[1,9,10] However, coating biomaterials display several drawbacks.[10–14] For instance, polyethylene glycol coatings are not readily recognized by the reticuloendothelial system, so their use with reticuloendothelial system-related diseases is limited.[10] The intrinsic toxicity of polyetherimide and its colloidal instability in a biological context are critical barriers to clinical entry.[11,12] Even when SPIONs are coated with natural polymers such as dextran, unfavorable effects may arise because of the common use of epichlorohydrin, a compound that is used as a cross-linker but that undergoes slow biodegradation.[9]

Polymeric micelles that are formed by the self-assembly of copolymers or polymers adopt core–shell structures that are suitable for drug delivery and imaging

contrast agents. Thus, intense interest exists in developing polymeric micelles as novel biomedical tools for theranostic applications.[1,15,16] Typically, copolymers are used to generate polymeric micelles; however, the costs and complexities associated with copolymer preparation raise serious concerns.[1,8]

In light of these disadvantages, recent studies have focused on developing MRI contrast agents using polymeric micelles that are derived from natural polymers or their nonchemically cross-linked derivatives.[13,15,17] Chitosan is a naturally occurring, low-cost cationic polysaccharide polymer.[18] Some chitosan derivatives modified by hydrophobic segments can self-aggregate into stable polymeric nanomicelles in aqueous solutions and form compact hydrophobic cores suitable for SPION encapsulation.[18–20] In most cases, chitosan derivatives used as drug delivery vehicles or MRI contrast agents are modified merely with hydrophilic or hydrophobic groups, or low molecular weight, water-soluble chitosans are employed.[18,21] While high molecular weight chitosan modified with hydrophilic groups is capable of self-aggregation and drug encapsulation, the complexity of synthesizing high molecular weight amphiphilic chitosans has limited their development and clinical applications.[18,19,22,23] Furthermore, chitosan derivatives can provide an abundance of reactive groups useful for the conjugation of targeting ligands and reporter moieties.[18] Therefore, a simple method for preparing targeted chitosan derivatives with encapsulated SPIONs as tumor-targeted MRI contrast agents is desirable.

Previously, we converted water-insoluble, high molecular weight chitosan to water-soluble N-palmitoyl chitosan (PLCS) by palmitoyl group conjugation in a one-step synthesis scheme and explored its potential for drug delivery.[15] PLCS self-assembled to form stable nanomicelles, and the compact core, which comprised long hydrophobic groups, encapsulated drug molecules and SPIONs efficiently.[15] Here, we prepared a novel tumor-targeted MRI contrast agent, folate-conjugated PLCS (FAPLCS), from high molecular weight chitosan that encapsulated SPIONs. Fourier transform infrared (FTIR) spectroscopy and ^{1}H nuclear magnetic resonance (NMR) were used to characterize the physicochemical properties of chitosan derivatives. Polymeric micelles composed of chitosan derivatives or FAPLCS/SPIONs were characterized by dynamic light scattering (DLS) and transmission electron microscopy (TEM). Cellular toxicities were evaluated in methylthiazolyldiphenyl-tetrazolium (MTT) assays. The tumor targeting ability of FAPLCS/SPIONs was determined in vitro and in vivo.

Materials and methods
Materials

Chitosan (molecular weight =23 kDa; 90%–95% deacetylated) was obtained from Shanghai Bio Science & Technology Co., Ltd. (Shanghai, People's Republic of China). Palmitic acid and acetic anhydride were purchased from Guangzhou Howei Chemical Co., Ltd. (Guangzhou, People's Republic of China). Folic acid was purchased from Sinopharm Chemical Reagent Co., Ltd. (Shanghai, People's Republic of China). SPIONs (Fe_3O_4; mean size: 5 nm) and MTT bromide were obtained from Sigma-Aldrich Co., Ltd. (St Louis, MO, USA). The reagent 1,1′-dioctadecyl-3,3,3′,3′-tetramethylindocarbocyanine perchlorate (DiI) was provided by Thermo Fisher Scientific (Waltham, MA, USA). All other chemicals and reagents used were of analytical grade. Female athymic mice (4–6 weeks old; 15–20 g) were obtained from the Experimental Animal Center of Southern Medical University (Guangzhou, People's Republic of China), housed in cages, and fed standard laboratory feed and water.

Synthesis and characterization of PLCS and FAPLCS

The synthesis of PLCS and FAPLCS was performed as described in Figure 1. In summary, 3.0 g chitosan was dissolved in 300 mL of acetic acid, precipitated with 55 mL of NaOH-saturated solution, collected by filtration, and washed with water until the pH reached 7. The chitosan was then dispersed in 100 mL of dimethyl sulfoxide (DMSO) with magnetic stirring, and 2.8 g palmitic anhydride was added dropwise to the mixture and allowed to react at 60°C for 8 hours. PLCS was obtained by precipitation with added acetone (500 mL), filtration, and washing the precipitate five times with a 1:1 solution of acetone and diethyl ether. The product was dried at 60°C for 48 hours under a vacuum for characterization and future use. The degree of palmitoyl substitution (PL-DS), defined as the number of the palmitoyl groups per 100 sugar residues of chitosan, was determined by ^{1}H NMR is the application of nuclear magnetic resonance in NMR spectroscopy with respect to hydrogen-1 nuclei within the molecules of a substance, in order to determine the structure of its molecules (density [d] =0.85 ppm) to H-2 protons (d =2.89 ppm) from chitosan.[15,24]

In this study, folic acid was conjugated to the PLCS with a degree of substitution (DS) of 10.6 as follows: 10 mL of folic acid/DMSO solution (0.005 g/mL) was mixed with 100 mL of aqueous PLCS solution (0.0091 g/mL). Subsequently, 0.04 g of 1-ethyl-3-(3-dimethylaminopropyl)-carbodiimide was added and the resulting mixture was stirred for 24 hours at room temperature. DMSO and unreacted folic acid were
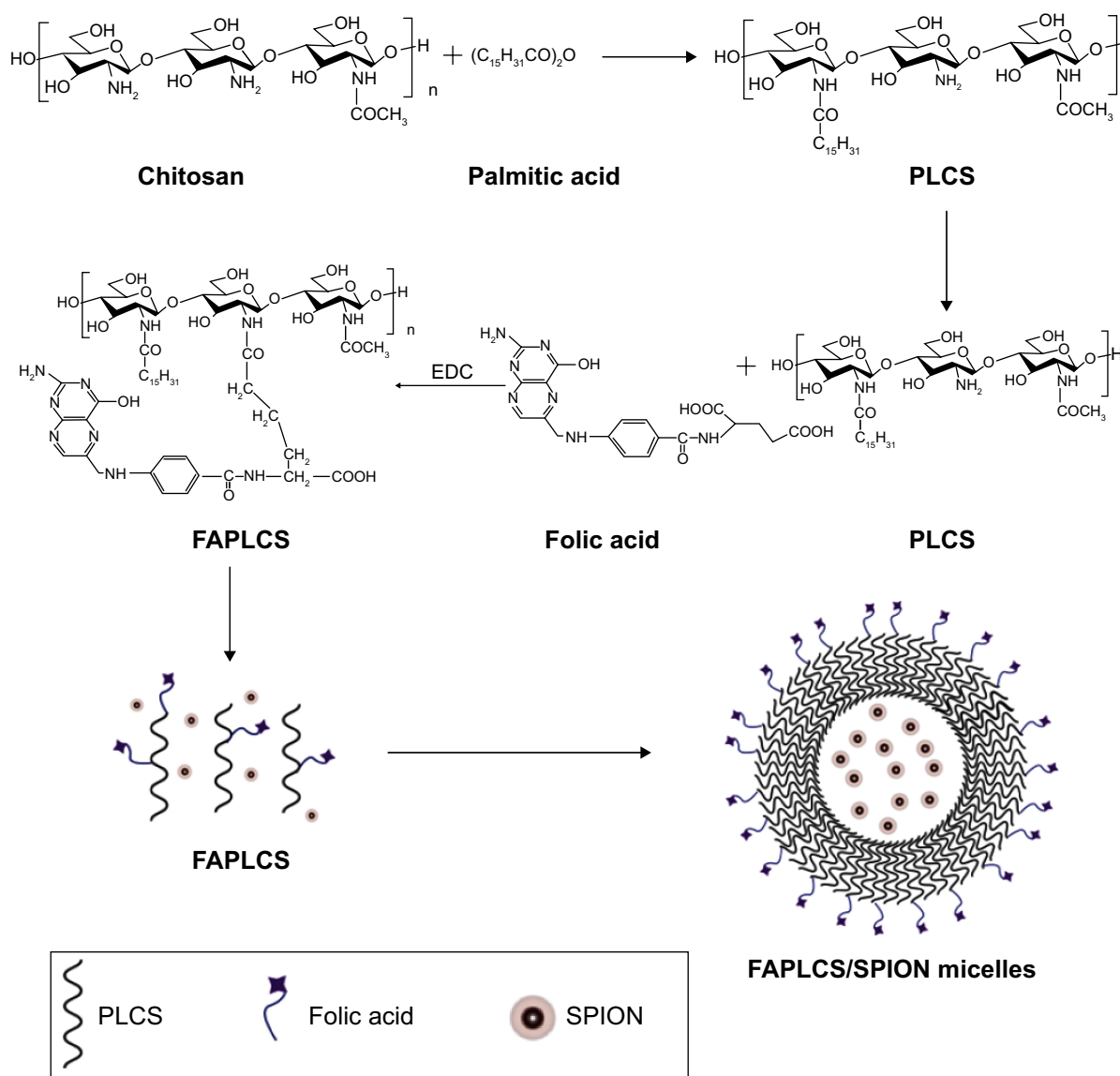
Figure 1 Synthesis of PLCS and FAPLCS and formation of FAPLCS/SPION micelles.
Abbreviations: PLCS, N-palmitoyl chitosan; FAPLCS, folate-conjugated N-palmitoyl chitosan; SPION, superparamagnetic iron oxide nanoparticle; 1-Ethyl-3-(3-dimethyl-aminopropyl)carbodiimide (EDC), water soluble carbodiimide usually obtained as the hydrochloride.

removed from the reaction mixture by dialysis against distilled water for 5 days (cutoff molecular weight =10 kDa) and then by freeze–drying to obtain FAPLCS. The degree of folate substitution (FA-DS) was calculated by ^{1}H NMR spectra using the ratio of $\delta_{6.64}$ benzene ring protons of folic acid to the $\delta_{3.37}$ sugar ring protons of chitosan.[15,24]

FTIR spectra were recorded on a Nicolet 6700 Infrared Detector (Thermo Fisher Scientific). Dry chitosan powder and its derivatives were mixed with KBr and then pressed to a plate for measurement. ^{1}H NMR spectra were acquired on an AV-600 MHz spectrometer (Bruker BioSpin GmbH, Karlsruhe, Germany) by using deuterated DMSO (DMSO-d6) as the solvent for FAPLCS and PLCS; chitosan was dissolved in a mixed solvent of CCl_3COOD and D_2O.

Preparation of FAPLCS/SPION and PLCS/SPION micelles

FAPLCS/SPION micelles were developed via self-aggregation in a dilute aqueous solution, as described previously.[15] In summary, 300 mg SPIONs was dispersed by sonication in a beaker containing 20 mL of ethanol, after which 500 mg FAPLCS was added. Distilled water was mixed slowly with the ethanol solution by sonication. This process resulted in FAPLCS solvation and self-aggregation and stable SPION encapsulation into FAPLCS micelles in aqueous solution. This solution was stored at room temperature for 4 hours to allow the ethanol to evaporate, and the SPION residue was collected by filtration (200 nm pore size). The beaker was washed three times with

distilled water, and the eluate was used to rinse the SPION filtrate. Washed SPIONs were dried and collected. The amount of total free SPIONs was determined by atomic absorption spectroscopy using a Varian SpectrAA 220Z (Varian Medical Systems, Inc., Palo Alto, CA, USA). The encapsulation efficiency of SPIONs in polymeric FAPLCS micelles was calculated using Equation 1:

$$EE\,(\%) = \frac{A - B}{A} \times 100\%, \qquad (1)$$

in which EE is the encapsulation efficiency, A is the total amount of reactant, and B is the total amount of free SPIONs, respectively.

In addition, polymeric PLCS/SPION micelles were prepared as described. Control polymeric PLCS and FAPLCS micelles were also prepared via self-aggregation in a dilute aqueous solution without added SPIONs. Hydrophobic DiI was loaded into FAPLCS/SPION polymeric micelles to trace the distribution of FAPLCS/SPIONs, as reported previously.[15]

Characterization of micelles
Particle size and size distribution
Average micelle size and size distributions were measured by DLS with a Zetaplus Zeta Potential Analyzer (Zetasizer 3000HS; Malvern Instruments, Malvern, UK).

Micelle surface charge determinations
Surface charges of polymeric micelles were determined with a Zetaplus Zeta Potential Analyzer at room temperature. Samples were diluted in triple-distilled water and sonicated for 2 minutes before measurement, and average readings were calculated from the average of six measurements.

Micelle surface morphologies
Micelle morphologies were investigated by TEM (JEM-2010F; JEOL, Tokyo, Japan). Suspensions of bare SPIONs, FAPLCS/SPION polymeric micelles, or PLCS/SPION polymeric micelles were dropped onto the surface of a 200 mesh copper grid with a carbon film; excess water was dried by absorption with filter paper, and samples were air-dried for 5 minutes at room temperature. Negative staining was achieved by the application of a methylamine tungstate negative stain for 2 minutes before TEM analysis.

Magnetic properties
The saturation magnetization of bare SPIONs, FAPLCS/SPIONs, and PLCS/SPIONs was measured by a superconducting quantum interference device (Quantum Design, Inc., San Diego, CA, USA) at 300 K between magnetic fields of −10 kOe to 10 kOe.

Relaxivity
T_2 relaxivity of the MRIs was obtained at room temperature using a clinical 3.0 Tesla MRI scanner (Signa Excite; GE Healthcare Bio-Sciences Corp., Piscataway, NJ, USA). Phantom MRI was performed at various iron concentrations of FAPLCS/SPIONs or PLCS/SPIONs, ranging from 0–0.24 mM in distilled water. For relaxivity measurements, the T_2-weighted scans were performed with repetition times of 2,400 ms and echo times ranging from 20–200 ms. In vitro, T_2 relaxivity values were calculated through curve fitting of relaxation times versus iron concentrations.

In vitro experiments
Cell cultures
Human lung cancer A549 cells and human cervical carcinoma HeLa cells were grown in Roswell Park Memorial Institute (RMPI) 1640 medium without folic acid (Thermo Fisher Scientific), and human L-O$_2$ hepatocytes were cultured in RMPI 1640 medium with folic acid (Thermo Fisher Scientific). All media were supplemented with 10% fetal bovine serum (FBS) (Thermo Fisher Scientific), and cells were maintained at 37°C and 5% CO$_2$ in a humidified incubator. HeLa, A549, and L-O2 hepatocytes were provided by the Chinese Academy of Cell Resource Center (Shanghai Institute of Biological Sciences, Chinese Academy of Sciences, Shanghai, People's Republic of China).

Cytotoxicity of FAPLCS/SPION micelles
L-O$_2$ hepatocytes were seeded in 96-well plates (Nunc, Roskilde, Denmark) at 8,000 cells/well. After 24 hours, the medium was aspirated and cells were incubated for an additional 24 hours in fresh medium containing FAPLCS/SPIONs (Fe concentration: 1.25 μg/mL, 2.5 μg/mL, 5 μg/mL, 10 μg/mL, or 20 μg/mL), SPIONs (Fe concentration: 1.25 μg/mL, 2.5 μg/mL, 5 μg/mL, 10 μg/mL, or 20 μg/mL), or FAPLCS (12.5 μg/mL, 25 μg/mL, 50 μg/mL, 100 μg/mL, or 200 μg/mL). At 24-hour intervals, cell viabilities were measured by MTT assays. To perform the MTT assays, cells were washed twice in phosphate buffer solution (PBS), and incubated for 4 hours in 20 μL of MTT and 100 μL of culture medium. Subsequently, the medium was removed, and the resulting purple formazan crystals were dissolved in DMSO. Absorbance was measured at 492 nm in a Multiscan

MK3 microplate reader (Thermo Fisher Scientific), and cell viabilities were calculated using Equation 2:

$$\text{Cell viability (\%)} = \frac{\text{Int}_s}{\text{Int}_{\text{control}}} \times 100\%, \qquad (2)$$

in which Int_s is the absorbance of cells incubated with a nanoparticle suspension, and $\text{Int}_{\text{control}}$ is the absorbance of cells incubated with the culture medium only.

Cellular uptake of FAPLCS/SPION micelles

Cells were stained with Prussian blue dye and visualized by light microscopy to track the internalization of FAPLCS/SPION micelles. Adherent HeLa and A549 cells in six-well plates (Nunc, Roskilde, Denmark) were washed twice with PBS, after which sterilized SPIONs, FAPLCS/SPIONs, or PLCS/SPIONs in 2 mL of RMPI 1640 without folic acid were added (final concentration: 0.4 mg iron/well). Alternatively, free folic acid (final concentration: 1.6 mg/L) was added to the cells for 30 minutes, after which FAPLCS/SPIONs (final concentration: 0.4 mg iron/well) in 2 mL of RMPI 1640 without folic acid were added. Control HeLa and A549 cells were incubated with culture medium alone. After 8 hours, wells were washed with PBS three times, fixed for 10 minutes in 0.5 mL of 4% paraformaldehyde (PFA) solution, and washed with PBS. Subsequently, each well was incubated for 20 minutes at 37°C with a 1:1 mixture of 2% potassium ferrocyanide and 2% hydrochloric acid solution that was prepared immediately before use. Next, the supernatant was removed, and wells were then washed three times with PBS. HeLa and A549 cells were stained with Prussian blue and examined under an optical microscope (BX51; Olympus, Tokyo, Japan).

To trace the intracellular distribution of FAPLCS/SPIONs, DiI was encapsulated in the hydrophobic core of FAPLCS/SPION micelles as a fluorescent probe. DiI-loaded polymeric micelles were sterilized by filtration through a 0.22 μm membrane. HeLa and A549 cells were cultivated at 37°C and 5% CO_2 in a chambered cover glass system (LAB-TEK®; Thermo Fisher Scientific) in their respective media. DiI-loaded FAPLCS/SPION solutions diluted in RMPI 1640 without folic acid were added to glass-bottom dishes. Following a 24-hour incubation period, adherent cells were washed twice with PBS, and DiI-loaded FAPLCS/SPIONs diluted in 2 mL RMPI 1640 without folic acid were added to each dish at a final concentration of 0.4 mg iron/well. After 8 hours, the wells were washed four times with PBS, fixed in 4% PFA for 10 minutes, and then washed twice with PBS. Nuclei were

stained with 4′,6-diamidino-2-phenylindole dihydrochloride (DAPI) for 30 minutes. Cells were washed twice with PBS and observed using a confocal laser-scanning microscope (Olympus FluoView FV1000; Olympus). The excitation and emission maxima used to detect DAPI bound to double-stranded DNA were 358 nm and 461 nm, respectively, while those for DiI were 549 nm and 565 nm, respectively.

In vivo experiments

The care and use of animals were conducted in compliance with the "Guide for the Care and Use of Laboratory Animals" protocol prepared by the Institute of Laboratory Animal Resources (National Research Council) and published by the National Academy Press.[25]

Targeting capacity of FAPLCS/SPION micelles in vivo

Thirty-six athymic mice were divided into six equal groups (number [n]=6), designated as groups A, B, C, D, E, and F. Groups A, B, and C were treated by subcutaneous injection of HeLa cells into the dorsal flank of left forethighs, whereas groups D, E, and F were prepared by subcutaneous injection of A549 cells. Athymic mice were anesthetized by intraperitoneal injection of pentobarbital when xenograft tumors grew to a diameter of 0.8 cm; these mice were then scanned with MRIs. After image acquisition, mice in groups A and D were injected with FAPLCS/SPIONs, those in groups B and E were injected with PLCS/SPIONs, and those in groups C and F were injected with SPIONs through the caudal vein at a dose equivalent to 2.0 mg Fe/kg of body weight. Subsequently, MRI scans for all groups were repeated after 1 hour, 4 hours, and 8 hours. All samples were measured by using a T_2-weighted spin-echo sequence (TR/TE =2,000/60, in which TR is the repetition time and TE is the echo time) for imaging, and quantitative analyses of MRIs were performed by a single experienced radiologist in blind fashion. Average signal intensities over regions of interest that were drawn on tumors were measured on MRI images. Background noise was measured in each image and its region of interest was placed 1 cm away from tumor peripheries. Signal-to-noise ratios and enhancement ratio of tumors on T_2-weighted MR in each group was calculated using Equations 3 and 4, respectively:

$$\text{SNR} = \frac{\text{SI}}{\text{SDN}}, \qquad (3)$$

in which SNR, SI, and SDN are the signal-to-noise ratio, signal intensity, and standard deviation of the noise, respectively.

$$ER (\%) = \frac{SNR\ post - SNR\ pre}{SNR\ pre} \times 100\%, \qquad (4)$$

in which ER is enhancement ratio, SNR pre and SNR post are the signal-to-noise ratios before and after the injection, respectively, of FAPLCS/SPIONs, PLCS/SPIONs, or SPIONs.

Following MRI scans, all athymic mice were deeply anesthetized by intraperitoneal injection of pentobarbital and euthanized by perfusion with 4% PFA via an open-chest, left cardiac ventricle puncture approach. The perfusion–fixation method enabled the removal of all blood from the animal body and allowed endovascular fixation. Subsequently, HeLa and A549 xenograft tumors were collected and embedded in paraffin.

Paraffin-embedded tumors were cut into 5 μm thick sections for histological analysis. The slide-mounted sections were deparaffinized, rehydrated, and reacted with 2% potassium ferrocyanide and 2% hydrochloric acid to visualize ferric iron particles by Prussian blue staining. Stained sections were washed and counterstained with nuclear fast red to confirm FAPLCS/SPIONs, PLCS/SPIONs, or SPIONs localization in tumors. Prussian blue staining results were assessed using an optical microscope (BX51; Olympus).

Biodistribution of FAPLCS/SPIONs in vivo

To study the distribution of FAPLCS/SPIONs by histology, six mice with HeLa xenograft tumors and six mice with A549 xenograft tumors were first injected intravenously with DiI-loaded FAPLCS/SPIONs at a dose equivalent to 2.0 mg Fe/kg of body weight. At 8 hours postinjection, mice were scanned with MRIs and euthanized. The ovaries, kidneys, lungs, intestines, spleens, livers, brains, HeLa tumors, and A549 tumors of mice were harvested and frozen. Tissues were cut into 5 μm thick sections for fluorescence analysis (BX51; Olympus). After 5–6 DiI fluorescent images were randomly acquired from one section per sample, the integrated optical densities of individual fluorescent images was measured by using an automated image analyzing system (Image-Pro Plus v6.0; Media Cybernetics, Rockville, MD, USA), and average integrated optical densities were calculated.

Statistical analysis

Comparisons between two groups were analyzed by the two-tailed Student's *t*-test. One-way analysis of variance (ANOVA) was used to evaluate particle size, the cytotoxicity of FAPLCS, and integrated optical densities. Two-way ANOVA was used to evaluate the cytotoxicity of FAPLCS/

SPIONs and SPIONs. Correlations between Fe concentrations and relaxivity times were drawn by linear regression analysis. Repeated-measures ANOVAs were performed to assess the enhancement ratio (ER) of signals in in vivo experiments. All statistical analyses were performed with SPSS software, version 12.0 (IBM Corporation, Armonk, NY, USA). Data are presented as the means ± standard deviations. Differences with *P*-values <0.05 were considered statistically significant.

Results and discussion
FAPLCS characterization

FTIR spectra of chitosan (Figure 2A), PLCS (Figure 2B), FAPLCS (Figure 2C), a 5% weight/weight (w/w) folic acid/PLCS mixture (Figure 2D), and folic acid (Figure 2E) are shown in Figure 2. The spectrum of unmodified chitosan exhibits a prominent amide II peak (N-H bending vibrations) at 1,597 cm^{-1} and a weak amide I peak (C=O stretching vibrations) at 1,655 cm^{-1}, which are attributed to the residual acetyl group of chitin. When the amine groups of chitosan are conjugated with palmitoyl groups, new peaks at 1,631 cm^{-1} and 1,518 cm^{-1} were observed and were assigned to carbonyl stretching of amide I peak and amide II peak, respectively. No peaks were observed at ~1,750 cm^{-1}, indicating that the conjugation reaction was highly selective toward N-acylation. The weak peak at 708 cm^{-1} and the enhancement of the peak intensity at 2,860–2,930 cm^{-1} confirmed that palmitoyl groups were grafted onto chitosan. Comparing PLCS and FAPLCS reveals the presence of a new peak in FAPLCS at 1,694 cm^{-1}, corresponding to a signal from the carbonyl group (C=O) of carboxylic acid of folic acid. While this peak is robust in the pure folic acid spectrum, the reduced signal in FAPLCS is due to the fractional DS with folate. However, the new peaks at 1,607 cm^{-1} (amide I peak) and 1,566 cm^{-1} (amide II peak) result from the introduction of new acrylamide and thereby confirm that PLCS is conjugated with folic acid. The peaks for carbonyl stretching of amides with pure folic acid appear at 1,606 cm^{-1} and 1,508 cm^{-1}, whereas the spectrum of a 5% w/w mixture of folic acid/PLCS is markedly different from that of FAPLCS. Most spectral peaks in the 1,100–1,700 cm^{-1} and 500–800 cm^{-1} regions with the folic acid/PLCS mixture are nearly identical to those of pure folic acid. Collectively, these data suggest that the palmitoyl and folate groups were successfully grafted onto the amino groups of chitosan.

Figure 3 displays the ^{1}H NMR spectra of chitosan (Figure 3A), folic acid (Figure 3B), PLCS (Figure 3C), and FAPLCS (Figure 3D). Proton assignments for chitosan in CCl$_3$COOD/D$_2$O (Figure 3A) were as follows: $\delta_{4.70}$ for H-1 overlaps D$_2$O; $\delta_{3.01}$ overlaps H-2; $\delta_{1.90}$ overlaps NHCOCH$_3$
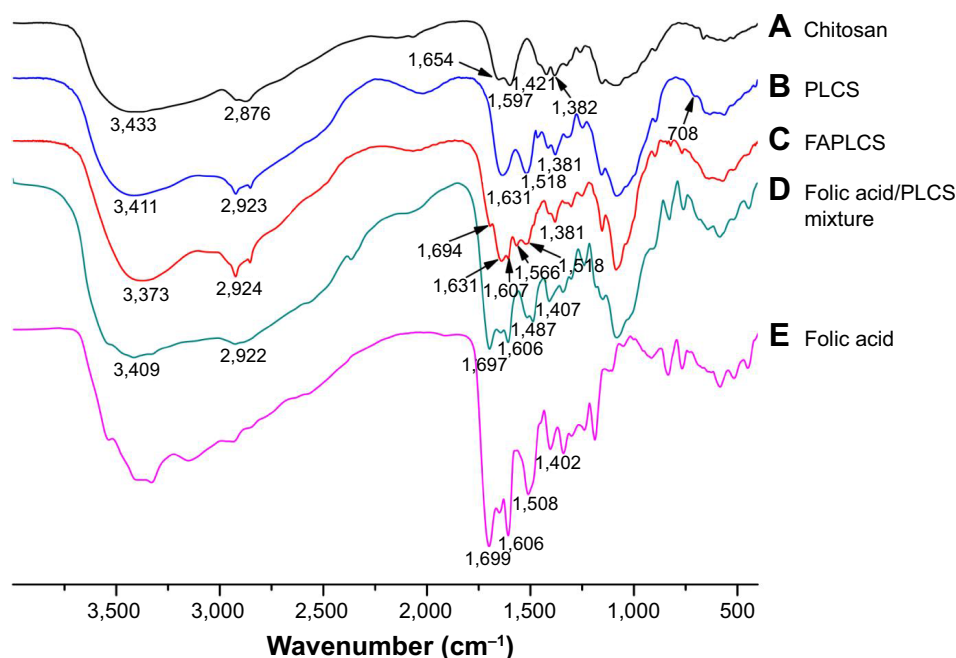
Figure 2 Fouriter transform infrared spectra of various agents.
Notes: Fourier transform infrared spectra of chitosan (**A**); PLCS (**B**); FAPLCS (**C**); folic acid/PLCS mixtures (5% w/w) (**D**); and folic acid (**E**).
Abbreviations: PLCS, N-palmitoyl chitosan; FAPLCS, folate-conjugated N-palmitoyl chitosan; w/w, weight/weight.

(the residual acetyl groups of chitosan); and $\delta_{3.47–3.74}$ correspond to the ring protons (H-3, 4, 5, 6, and 6′). Proton assignments for PLCS in DMSO (Figure 3C) were reported in our previous study[15] as: $\delta_{0.85}$ = CH$_3$ (palmitoyl terminus); $\delta_{1.23}$ = CH$_2$ (palmitoyl); $\delta_{1.48}$ = CH$_2$ (palmitoyl deshielded by carbonyl, β to carbonyl); $\delta_{1.84}$ = CH$_2$ (residual acetyl groups); and $\delta_{2.06}$ = CH2 (palmitoyl deshielded by carbonyl, α to carbonyl). The signal at $\delta_{5.64}$, seen in the FAPLCS spectrum but not in the PLCS spectrum, is attributable to the N-H bond associated with folic acid, and the prominent signals at $\delta_{5.53–8.85}$, $\delta_{4.32–4.47}$, and $\delta_{1.91–2.38}$ correspond to the protons of folic acid (Figure 3D). These results provide further evidence that palmitoyl and folate groups were successfully grafted onto chitosan.

Determining the ratio of palmitoyl methyl protons ($\delta_{0.85}$) to H-2 protons ($\delta_{3.01}$) of chitosan in ^{1}H NMR spectra enables determination of the PL-DS. The FA-DS was determined by using the ratio of benzene ring protons at $\delta_{6.64}$ of folic acid to the $\delta_{3.37}$ sugar ring protons of chitosan. In this study, the PL-DS and FA-DS were 10.60% and 0.48%, respectively.

Size distribution

PLCS is composed of hydrophobic groups and a chitosan backbone. In addition to this basic structure, FAPLCS also has tumor-targeting folate groups. In aqueous solutions, the hydrophobic palmitoyl groups of PLCS or FAPLCS can spontaneously form rigid hydrophobic cores, while the hydrophilic chitosan backbones form an outer shell, resulting

in the fabrication of polymeric micelles.[22] During the process of micelle formation, hydrophobic SPIONs can be encapsulated by the hydrophobic cores of micelles, and tumor-targeting groups may be conjugated to their surfaces.

The mean diameter and polydispersity index of polymeric micelles were measured by using DLS. As shown in Table 1, Figure 4 and Figure S1, the mean diameters of FAPLCS (Figure 4A) and PLCS micelles were 121±3.7 nm and 89.90±4.90 nm, respectively. Because PLCS is modified with folic acid, the mean size of FAPLCS micelles is larger than that of PLCS. Likewise, the average diameters of FAPLCS/SPION (Figure 4B) and PLCS/SPION micelles were found to be 136.60±3.90 nm and 120.90±3.60 nm, respectively. No significant differences were observed between the mean diameters of either polymeric micelles (*P* not significant), even though they have larger diameters than their counterparts without encapsulated SPIONs (*P*<0.05). The polydispersity index of polymeric micelles was small and uniform, indicating that the size distribution of the micelles was good. The majority of solid tumors show a vascular pore cut-off size between 380 nm and 780 nm;[26] hence, particles below the cut-off size can readily traverse the endothelial barrier. The use of appropriately sized SPIONs is critical in clinical testing, especially for tumor-targeted MRI contrast agents. SPION-based tumor-targeting MRI contrast agents with diameters of 100–200 nm may be ideal for avoiding rapid clearance by the mononuclear phagocytic system (MPS) and
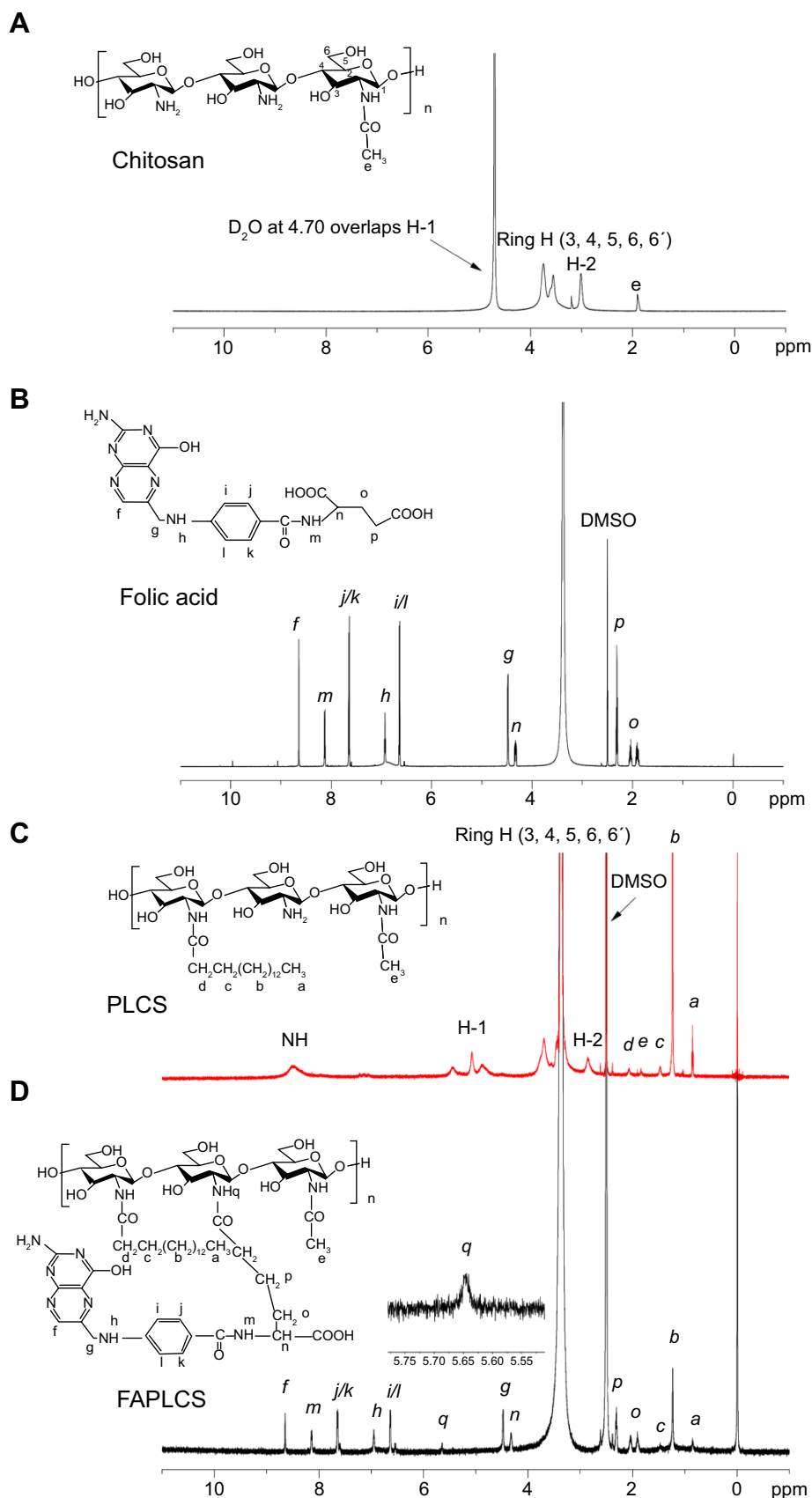
Figure 3 ¹H NMR spectra of various agents.
Notes: ¹H NMR spectra of chitosan in CCl₃COOD/D₂O (**A**); folic acid in DMSO (**B**); PLCS in DMSO (**C**); and FAPLCS in DMSO (**D**).
Abbreviations: PLCS, N-palmitoyl chitosan; FAPLCS, folate-conjugated N-palmitoyl chitosan; NMR, nuclear magnetic resonance; DMSO, dimethyl sulfoxide.

Table 1 Properties of various types of micelles in deionized water

Micelles	Particle size (nm)	Polydispersity index	EE (%)	Zeta potential (mV)
FAPLCS/SPION	136.60±3.90[a,b,c]	0.24±0.02	84.60±3.00	52.10±0.90
PLCS/SPION	120.90±3.60[a]	0.22±0.02	83.40±2.80	51.90±1.80
FAPLCS	121.70±3.70[a]	0.25±0.04		50.50±3.10
PLCS	89.90±4.90	0.28±0.05		51.30±2.50

Notes: Number =6 number of samples in each category; [a]significant at $P<0.05$ in comparison with PLCS; [b]significant at $P<0.05$ in comparison with FAPLCS; [c]significant at $P<0.05$ in comparison with PLCS/SPION. The figures are presented as mean value ± standard deviation.
Abbreviations: EE, encapsulation efficiency; FAPLCS, folate-conjugated N-palmitoyl chitosan; SPION, superparamagnetic iron oxide nanoparticle; PLCS, N-palmitoyl chitosan.

may reduce in vivo toxicity by limiting undesirable migration to other areas in the body.[27–29] Thus, the size of FAPLCS/SPION micelles generated in this study would be suitable for use as tumor-targeted MRI contrast agents.

Micelle surface charge

Zeta potential values of micelles are presented in Table 1 and Figure 4. The mean zeta potential values of FAPLCS/SPION and PLCS/SPION micelles were 52.10±0.90 mV and 51.90±1.80 mV, respectively. No significant difference in the mean zeta potential values between micelle types was observed (P not significant). The zeta potential values were positive because the surface of the micelles of cationic chitosan is positively charged. The high zeta values observed (>50 mV) indicated that FAPLCS/SPION and PLCS/SPION micelles possessed high electric charges on their surfaces, which could prevent micelle aggregation in water and maintain high stability because of strong repellent forces between micelles.

Surface morphology and SPION encapsulation efficiency

The morphology of FAPLCS/SPION micelles (Figure 4A), FAPLCS micelles (Figure 4B), bare SPIONs (Figure S1A), PLCS/SPION micelles (Figure S1B), and PLCS micelles (Figure S1C) is depicted by TEM images. All polymeric micelles were spherical and uniform in shape. No aggregation was observed in aqueous solutions, a result that was later confirmed in DLS experiments. Clustering of multiple dark points, created by SPION encapsulation, was evident with FAPLCS/SPION micelles (Figure 4B). In contrast, vacant micelles were white in color and lacked dark clusters, as shown with TEM of FAPLCS micelles (Figure 4A). Table 1 shows that the encapsulation efficiencies of SPIONs were 84.60%±3.00% in FAPLCS/SPION micelles and 83.40%±2.80% in PLCS/SPION micelles, in agreement with a previous report demonstrating that FAPLCS and PLCS micelles had similar effective loading efficiencies.[30]
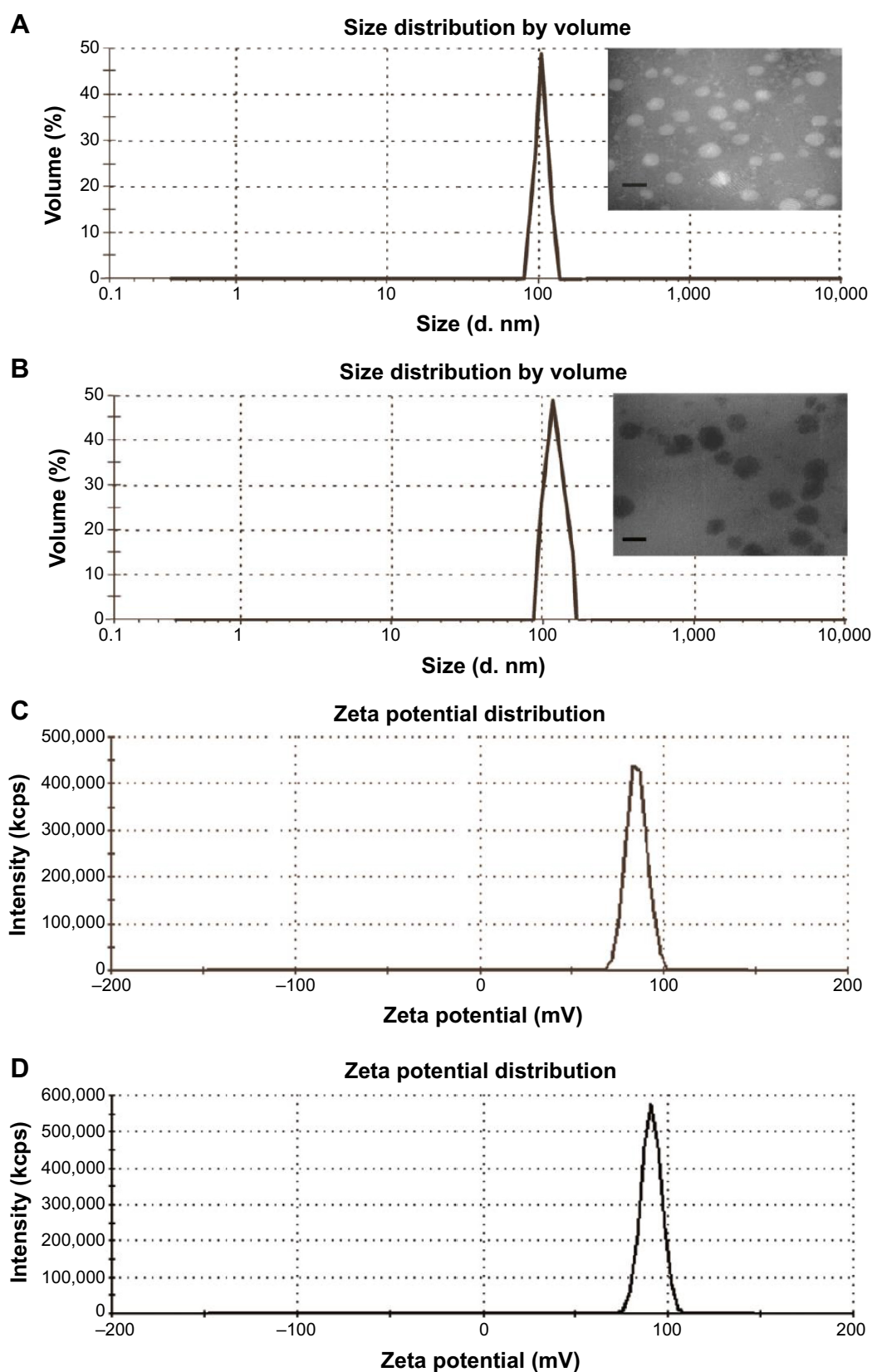
SPION encapsulation inside the hydrophobic cores of micelles covers the hydrophobic surface of SPIONs, thereby preventing the adsorption of blood proteins on SPION surfaces and phagotrophy by the MPS[27,28] and prolonging the circulation times of MRI contrast agents in blood for enhanced tumor-targeting efficiency.[31]

Magnetic properties of polymeric micelles

The preservation of favorable magnetic properties of SPIONs is a determining factor of their utility as contrast enhancement agents in clinical MRIs. A superconducting quantum interference device magnetometer was used to investigate the magnetic properties of bare SPIONs, FAPLCS/SPION micelles, and PLCS/SPION micelles. The magnetic hysteresis loops of bare SPIONs, FAPLCS/SPIONs, and PLCS/SPIONs are shown in Figure 5. In 1:300 K, the saturation magnetization (Ms) values of SPIONs, FAPLCS/SPIONs, and PLCS/SPIONs were 42.4 emu/g, 14.4 emu/g, and 12.6 emu/g, respectively. The magnetization curves of micelles indicated that they are superparamagnetic in 1:300 K because the net magnetization returned to 0 without an external field.[32] Owing to the decrease in their SPION content, the Ms of SPIONs was markedly reduced after encapsulation by polymeric micelles, although FAPLCS/SPIONs still exhibited promising superparamagnetic behavior. Similar Ms changes were observed in previous studies using SPIONs encapsulated in chitosan derivatives that stably retained the magnetic properties of SPIONs.[33,34] These results indicate that FAPLCS/SPIONs are potentially useful MRI contrast agents.

T$_2$ relaxivity

Contrast agent sensitivity, T$_2$ (spin–spin) relaxation times, and the generation of negative contrast enhancement images are important factors for obtaining high quality MRIs in vivo. Thus, FAPLCS/SPION and PLCS/SPION micelles were studied in vitro at increasing concentrations with T$_2$-weighted MRIs to determine their sensitivities and T$_2$-enhancing

A

Size distribution by volume

B

Size distribution by volume

C

Zeta potential distribution

D

Zeta potential distribution

Figure 4 Size and zeta potential distribution of FAPLCS and FAPLCS/SPIONs.
Notes: The mean diameter of FAPLCS was 121.70±3.70 nm; the insert shows TEM images of FAPLCS micelles (**A**). The mean diameter of FAPLCS/SPIONs was 136.60±3.90 nm; the insert shows FAPLCS/SPION micelles (**B**). The mean zeta potential value of FAPLCS was 50.50±3.10 mV (**C**). The mean zeta potential value of FAPLCS/SPIONs was 52.10±0.90 mV (**D**). Scale bar =100 nm for all inserts.
Abbreviations: FAPLCS, folate-conjugated N-palmitoyl chitosan; SPION, superparamagnetic iron oxide nanoparticle; TEM, transmission electron microscopy.
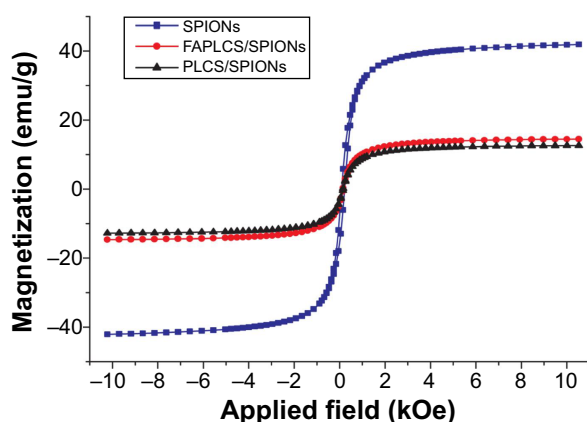
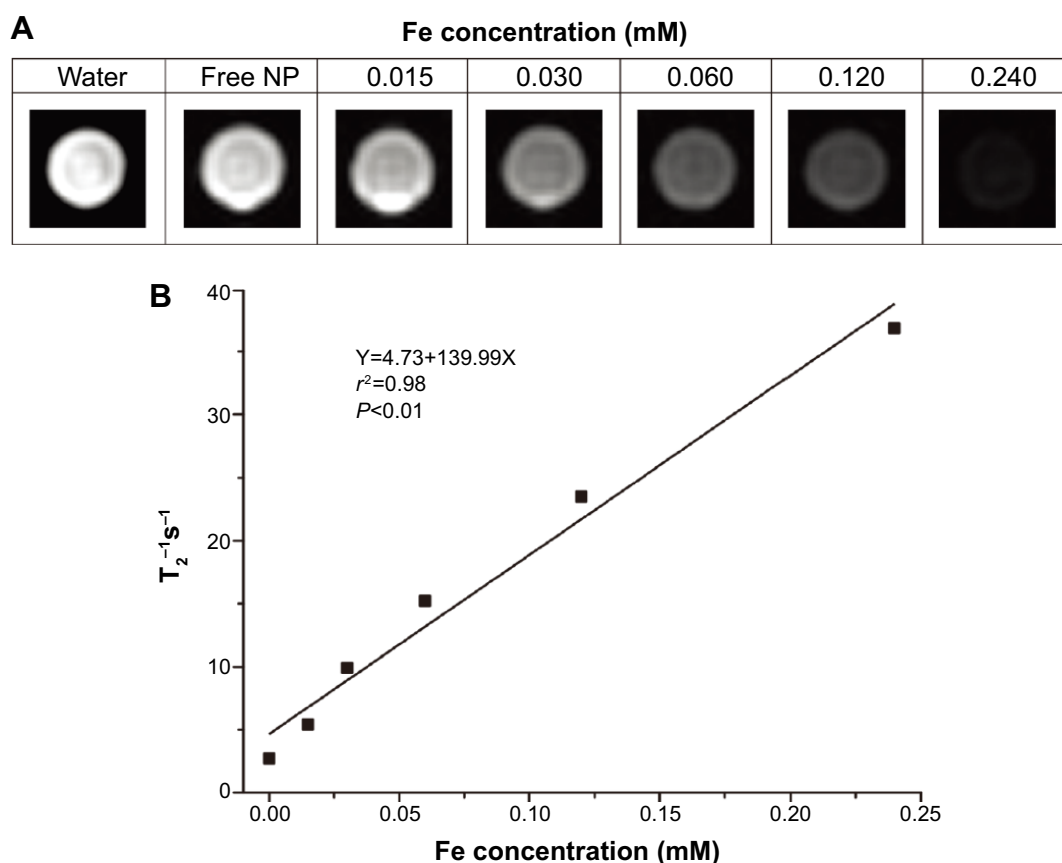**Figure 5** SQUID measurements of SPIONs, FAPLCS/SPIONs, and PLCS/SPIONs at 300 K.
Abbreviations: SPION, superparamagnetic iron oxide nanoparticle; FAPLCS, folate-conjugated N-palmitoyl chitosan; PLCS, N-palmitoyl chitosan; SQUID, superconducting quantum interference device.

abilities. The presence of FAPLCS/SPIONs (Figure 6A) and PLCS/SPIONs in water induced signal losses in T_2-weighted MRI images similar to that observed with increased iron concentration.[32] The shortened T_2 relaxation times of both FAPLCS/SPION micelles (Figure 6B) and PLCS/SPION

micelles were well correlated by linear regression analysis within the range of iron concentrations studied (0.015–0.24 mM) and displayed the characteristic SPION property of shortened T_2 relaxation times.[32] T_2 relaxivity, calculated as the slope of T_2^{-1} versus iron concentration, was 139.99 mM^{-1} s^{-1} and 135.56 mM^{-1} s^{-1} for FAPLCS/SPION micelles and PLCS/SPION micelles, respectively. These micelles have T_2 relaxivity values that are similar to or larger than the SPIO-dextran particles currently used in clinical diagnoses.[35] These results indicate that FAPLCS/SPION micelles and PLCS/SPION micelles have strong sensitivity and potential for use as MRI contrast agents.

Cytotoxicity

Potential toxic effects of bare SPIONs is a natural concern when used in medical applications. The MTT assay was employed to assess the cytotoxicity of FAPLCS/SPION micelles and the cell viability of treated L-O$_2$ hepatocytes. Minimal cellular cytotoxicity was observed when L-O$_2$ hepatocytes were incubated for 24 hours with FAPLCS/SPION micelles at high Fe concentrations (10–20 μg/mL); however, significant

Figure 6 T_2-weighted MRI images of FAPLCS/SPIONs at various Fe concentrations.
Notes: T_2-weighted MRI images of FAPLCS/SPIONs (**A**). T_2 relaxation rates T_2^{-1}(s^{-1}) as a function of Fe concentration (mM) in FAPLCS/SPIONs (**B**).
Abbreviations: NP, nanoparticle; MRI, magnetic resonance imaging; FAPLCS, folate-conjugated N-palmitoyl chitosan; SPION, superparamagnetic iron oxide nanoparticle.

cytotoxicity was observed when $L-O_2$ cells were treated with bare SPIONs at the same concentrations (Figure 7A). The viability of cells that were exposed to FAPLCS/SPION micelles at 20 µg/mL Fe concentration was 82.51%±5.31%. It is approximately twofold higher than that observed with bare SPIONs at the same Fe concentration ($P < 0.05$). Most cells cocultured with FAPLCS micelles were viable and similar to control cells (P not significant; Figure 7B). These results demonstrate that SPION encapsulation with FAPLCS micelles effectively reduces SPION cytotoxicity and suggests that FAPLCS polymeric micelles have excellent biocompatibility and are safe for SPION encapsulation.

Targeting capacity of FAPLCS/SPION micelles in vitro

The in vitro targeting capacity of FAPLCS/SPION micelles was evaluated using a cellular uptake assay and was compared to the capacities of PLCS/SPION micelles and SPIONs. HeLa cells (positive for folate receptor [FR] expression) and A549 cells (negative for FR expression) were incubated separately for 8 hours with FAPLCS/SPION micelles, PLCS/SPION micelles, SPIONs, and free folic acid-combined FAPLCS/SPION micelles. Subsequently, Prussian blue staining was performed to determine targeting capacities of these reagents toward FR-positive HeLa cells. As controls, HeLa and A549 cells were maintained in culture in the absence of micelles or nanoparticles and processed in the same manner. Figure 8A shows optical microscope images of HeLa and A549 cells incubated with or without micelles or nanoparticles, and treated with Prussian blue staining. Blue staining was observed in HeLa cell membranes and as punctate patterns in the cytoplasm in most HeLa cells incubated with FAPLCS/SPION micelles. In contrast, marginal blue staining and sporadic blue cytoplasmic spots were observed in a low percentage of HeLa cells incubated with PLCS/SPION micelles, SPIONs, free folic acid combined FAPLCS/SPION micelles, A549 cells incubated with FAPLCS/SPION micelles, PLCS/SPION micelles, SPIONs, and free folic acid-combined FAPLCS/SPION micelles. No blue staining was observed in control cells. These results provide strong evidence suggesting that FAPLCS/SPION micelles target FRs on the surface of HeLa cells, which may internalize FAPLCS/SPION micelles by FR-mediated endocytosis.[36] Low levels of nonspecific endocytosis may be responsible for the uptake of A549 cells.

To confirm that FAPLCS/SPION micelles target FRs in vitro, HeLa cells and A549 cells were treated with DiI-loaded FAPLCS/SPION micelles for 8 hours and imaged with a confocal laser scanning microscope (Figure 8B). Red fluorescent intensities in FR-positive HeLa cells were stronger than those in FR-negative A549 cells (Figure 8B). Thus, the goal of increasing specificity and sensitivity in detecting cancer cells with FR overexpression on their surfaces may be achieved by molecular imaging using folate-bearing contrast agents based on FAPLCS/SPION micelles.

Active targeting capacity of FAPLCS/ SPION micelles in vivo

The in vivo targeting efficacies of FAPLCS/SPION micelles, PLCS/SPION micelles, and SPIONs in MRIs were investigated in HeLa and A549 xenograft tumor-bearing mice. The T_2-weighted MRIs of the central region of HeLa and A549 cell tumors were acquired before and at 1 hour, 4 hours, and 8 hours after injection of FAPLCS/SPION micelles, PLCS/SPION micelles, or SPIONs via the caudal vein.
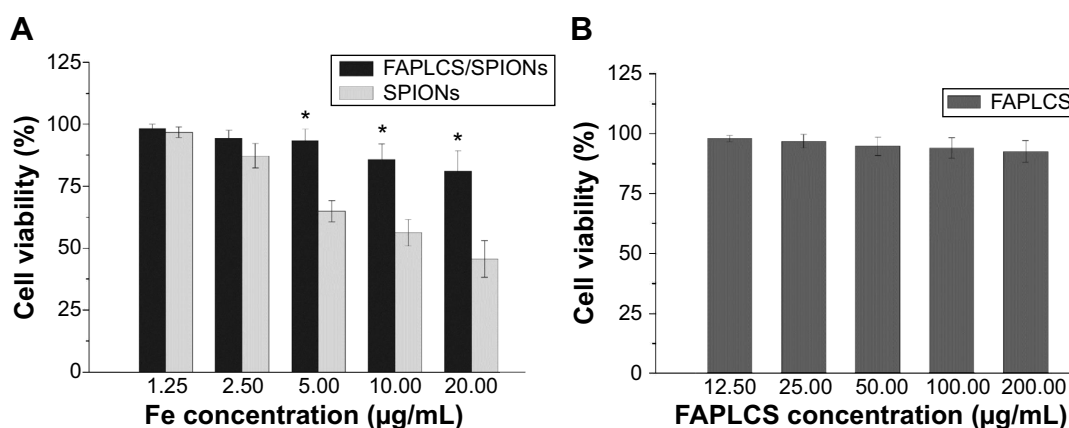

Figure 7 Dose-dependent in vitro viability of $L-O_2$ hepatocytes with various contrast agents.
Notes: Dose-dependent in vitro viability of $L-O_2$ hepatocytes incubated with FAPLCS/SPION micelles and bare SPIONs at 24 hours posttreatment (**A**). Dose-dependent in vitro viability of $L-O_2$ hepatocytes treated with FAPLCS micelles after 24 hours in culture (**B**).
Abbreviations: FAPLCS, folate-conjugated N-palmitoyl chitosan; SPION, superparamagnetic iron oxide nanoparticle.
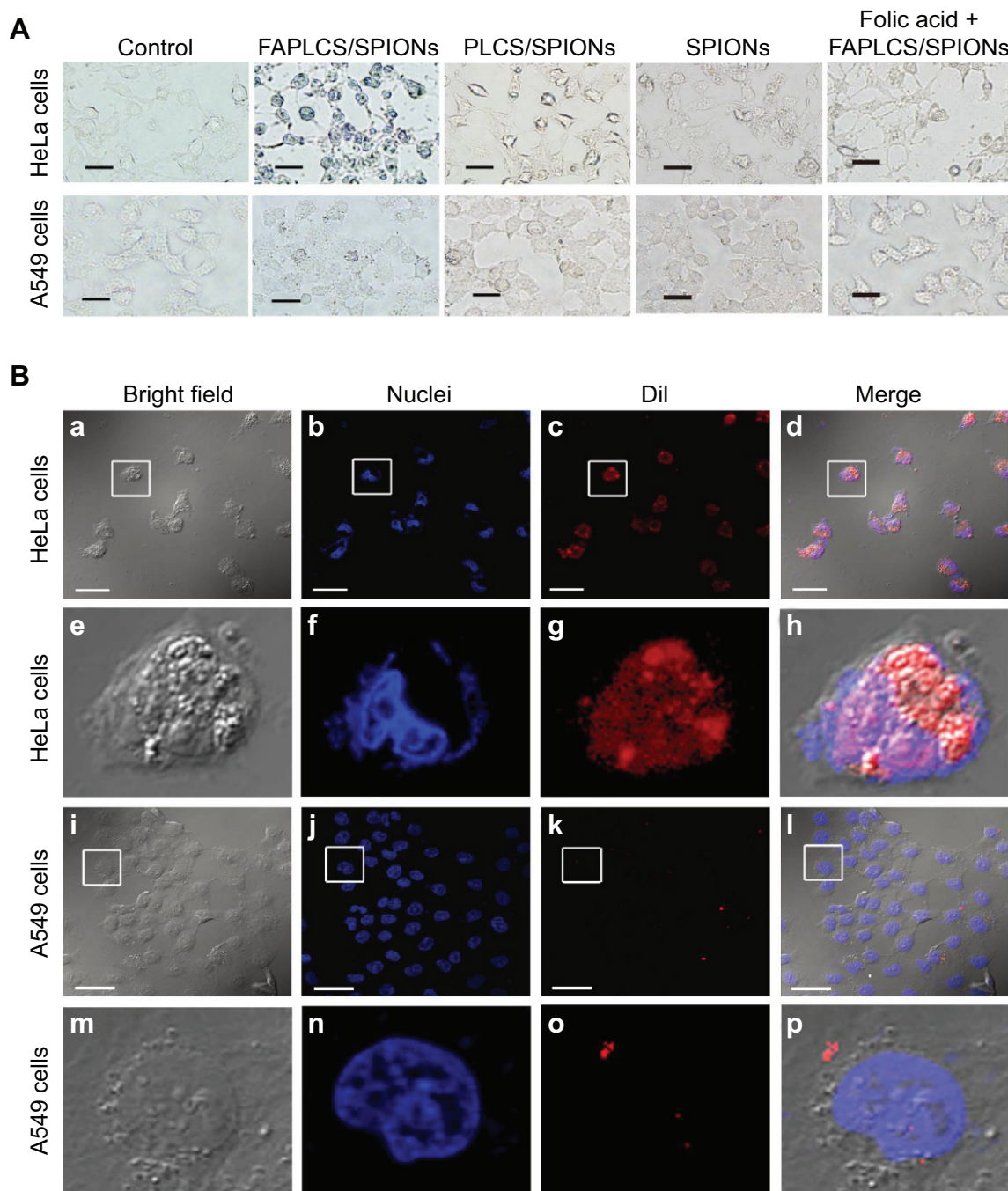
Figure 8 HeLa cells and A549 cells treated with various contrast agents.
Notes: In vitro Prussian blue staining images of controls of HeLa cells and A549 cells and images of these cells after treatment with FAPLCS/SPIONs, PLCS/SPIONs, SPIONs, and free folic acid-combined FAPLCS/SPIONs (**A**). Confocal laser scanning microscopy of cells treated with DiI-loaded FAPLCS/SPIONs: HeLa (a–d; corresponding high magnification images shown in e–h) and A549 (i–l; corresponding high magnification images shown in panels m–p) (**B**). Scale bar =20 μm.
Abbreviations: FAPLCS, folate-conjugated N-palmitoyl chitosan; SPION, superparamagnetic iron oxide nanoparticle; PLCS, N-palmitoyl chitosan; DiI, 1,1′-dioctadecyl-3,3,3′,3′-tetramethylindocarbocyanine perchlorate.

Compared to the baseline values, signal intensities in T_2-weighted images with established HeLa cell tumors were lower 1 hour after the administration of FAPLCS/SPION micelles, and the rate of decrease gradually minimized over time (Figure 9A; $P<0.05$). This effect may be attributable to FR overexpression in HeLa tumor cells. In such a case,

FAPLCS/SPION micelles would quickly bind FRs on the surface of HeLa tumor cells and become internalized through receptor-mediated endocytosis. The D-glucosidic linkages of FAPLCS in intracellular FAPLCS/SPION micelles are predicted to be hydrolyzed and, thus, result in the release of SPIONs, the degradation of SPIONs by hydrolytic enzymes,
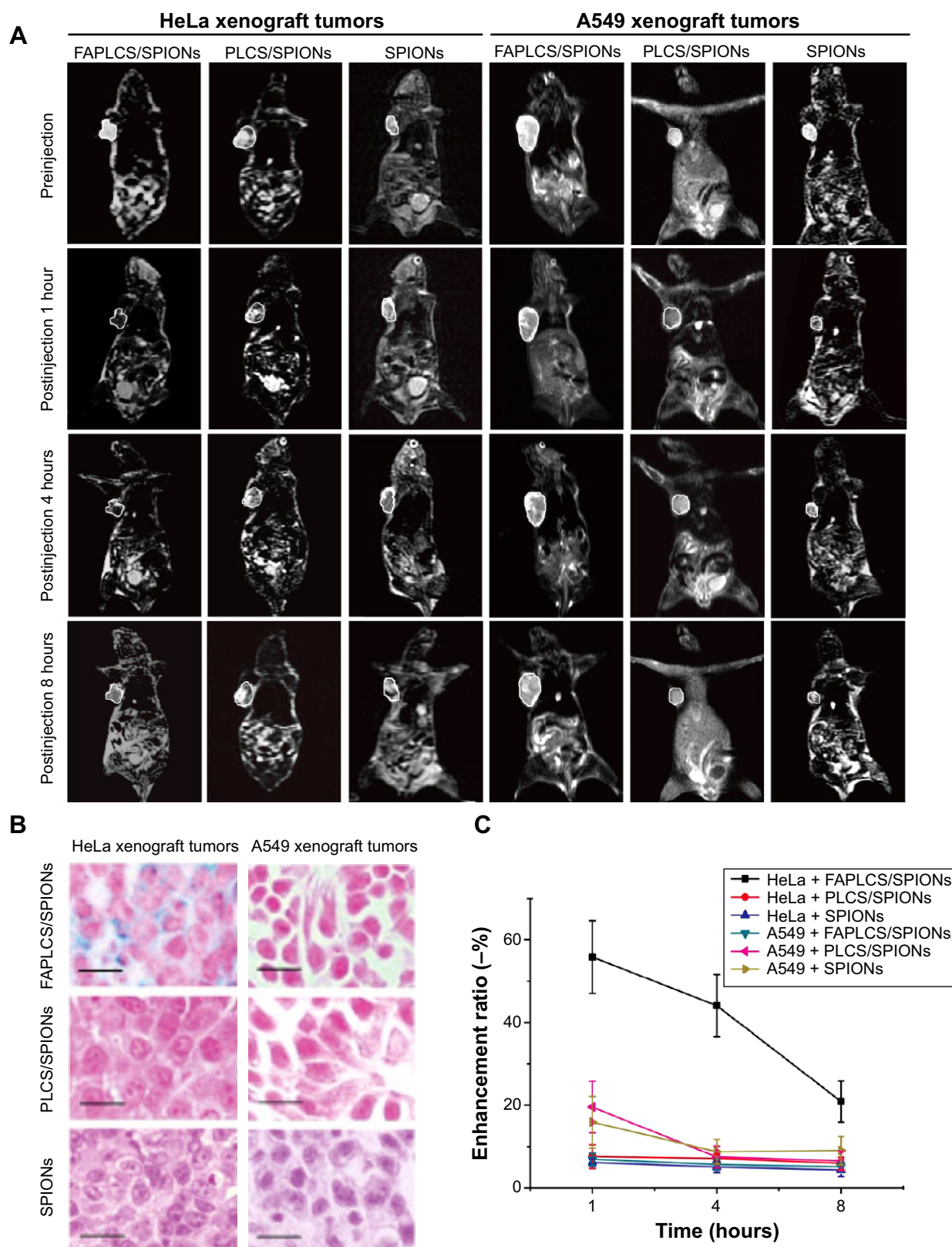
Figure 9 Images of xenograft tumors treated with various contrast agents.

Notes: T_2-weighted MRI images of central regions of HeLa xenograft tumors and A549 xenograft tumors before and at 1 hour, 4 hours, and 8 hours after injection of FAPLCS/SPIONs or PLCS/SPIONs (**A**). Images of Prussian blue-stained and nuclear fast red-counterstained HeLa and A549 xenograft tumor sections after intravenous injection of FAPLCS/SPIONs and PLCS/SPIONs in mice; scale bar =20 μm (**B**). T_2-weighted MRI signal intensity changes in regions of interest (**C**).

Abbreviations: FAPLCS, folate-conjugated N-palmitoyl chitosan; SPION, superparamagnetic iron oxide nanoparticle; PLCS, N-palmitoyl chitosan; MRI, magnetic resonance imaging.
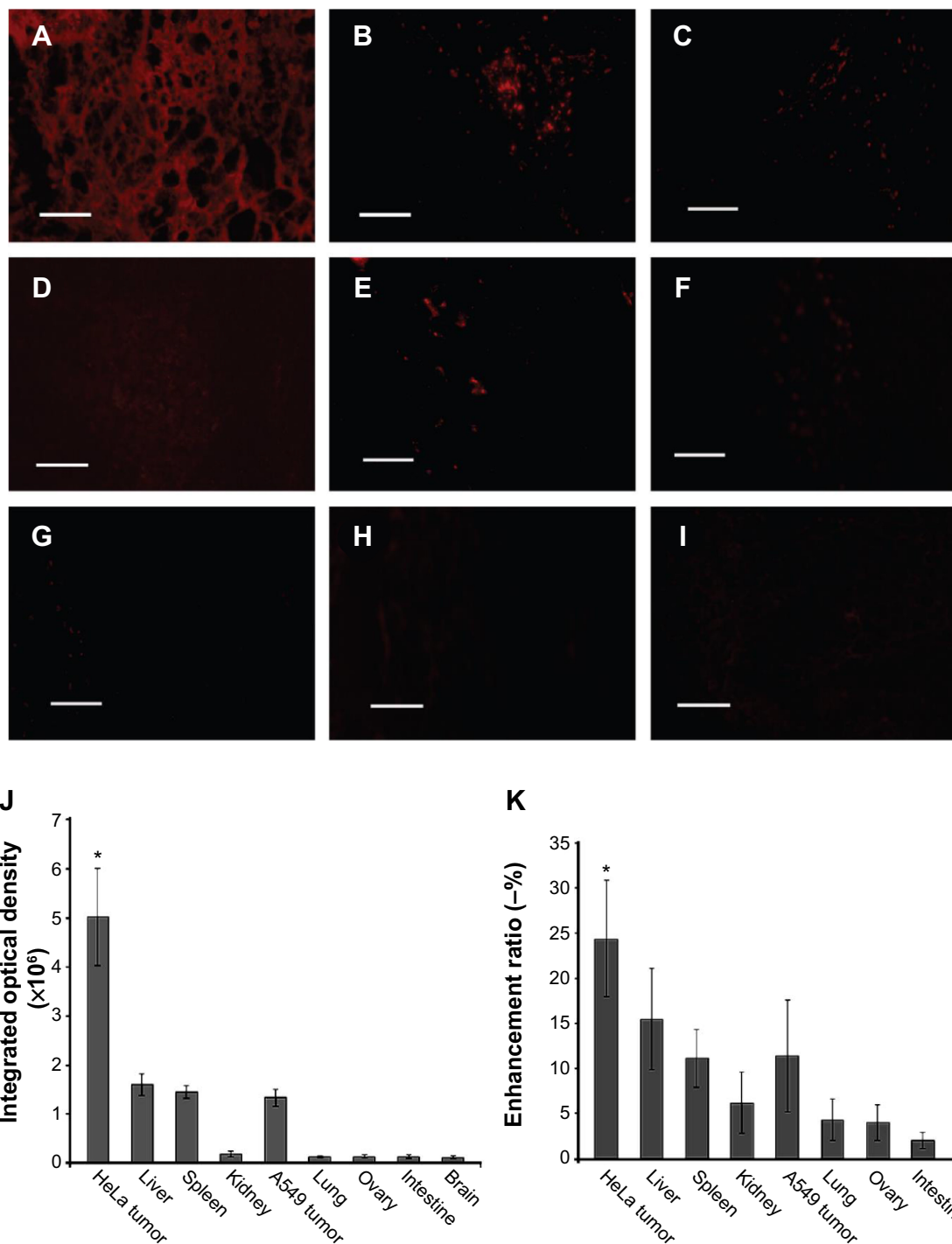
Figure 10 Fluorescence images and optical properties of tissue sections from a HeLa xenograft tumor.
Notes: Fluorescence images of tissue sections from a HeLa xenograft tumor (**A**), liver (**B**), spleen (**C**), kidney (**D**), a A549 xenograft tumor (**E**), lung (**F**), ovary (**G**), intestine (**H**), and brain (**I**). Integrated fluorescence optical densities (**J**) and enhancement ratios (**K**) after injection of FAPLCS/SPIONs are shown. Scale bar =100 μm.
Abbreviations: FAPLCS, folate-conjugated N-palmitoyl chitosan; SPION, superparamagnetic iron oxide nanoparticle.

the reduced accumulation of FAPLCS/SPION micelles in tumor cells, and reduced T_2 relaxivity.[18,34,37] Therefore, SPIONs accumulation in tumor cells shortens T_2 relaxation times and thereby results in decreased MRI signal intensities[38] and darkened tumor images in T_2-weighted MRI images.

As expected, no significant losses in signal intensity were observed in HeLa cell tumor-bearing mice after administration of PLCS/SPION micelles or SPIONs, or in A549 cell tumor-bearing mice after administration of FAPLCS/SPION micelles, PLCS/SPION micelles, or SPIONs

(Figure 9A and C; P not significant). As found in the in vitro study, nonspecific endocytosis occurred in A549 xenograft tumors incubated with FAPLCS/SPION micelles and with A549 and HeLa cells incubated with PLCS/SPIONs or SPION micelles. A reasonable explanation for the difference between the in vivo and in vitro models is that the rate of endocytosis is too slow to cause a significant loss in signal intensity of MRIs of tumors without receptor-mediated endocytosis of folate.

To test this possibility, the in vivo targeting efficacy of FAPLCS/SPION micelles, PLCS/SPION micelles, and SPIONs in mice bearing either the HeLa tumor line or A549 tumor line was studied by Prussian blue staining of tumors taken at 8 hours after administration. Significant cytoplasmic blue staining was observed in most HeLa cells after the injection of FAPLCS/SPION micelles (Figure 9B). However, micelle accumulation was barely observable in HeLa cells administered PLCS/SPION micelles or SPIONs (Figure 9B). The same observations were made in A549 cells treated with FAPLCS/SPION micelles, PLCS/SPION micelles, or SPIONs (Figure 9B). These results suggest that FAPLCS/SPION micelles can serve as efficient MRI contrast agents for active targeted imaging of FR-positive tumors.

Biodistribution of FAPLCS/SPION micelles in vivo

The biodistribution of FAPLCS/SPION micelles in mice bearing HeLa tumors and in those bearing A549 tumors was studied by fluorescence microscopy. Tissues were collected 8 hours after the administration of fluorescently labeled FAPLCS/SPION micelles. Among the samples, the highest levels of fluorescence intensity were observed in HeLa cell tumors (Figure 10A). Specific types of tissue showed high fluorescence intensities; these are the tissue types, which are listed in descending order of intensity: the liver; the spleen; and the A549 tumor (Figure 10B–D). However, fluorescence intensity levels in kidney, lung, ovary, intestine, and brain tissue (Figure 10E–G) were significantly lower ($P<0.05$). Although fluorescence intensity levels in HeLa derived tumors were much higher than those observed in other organs, similar biodistribution patterns have been reported previously.[22,34,39]

The greatest obstacle for tumor-targeted MRI is perhaps the accumulation of adequate SPIONs at target sites to produce sufficient contrast for MRI images.[38] In addition to approaches using ligand-conjugated and antibody-conjugated SPIONs, a promising strategy to increase SPION accumulation levels at target sites and improve targeting efficiency

is to decrease the SPION size because SPIONs >200 nm in diameter may be rapidly eliminated from the body by the MPS,[27,28] mainly in the liver and spleen.[27] However, particles <100 nm in diameter may cause unexpected migration and accumulation in the body and thereby cause toxic effects, such as acute liver damage.[29] The novel FAPLCS/SPIONs in this study are approximately 136.55±3.99 nm in diameter in aqueous solution, which should be ideal for tumor-targeting MRI scans.

Summary

In this study, we developed novel, biocompatible FAPLCS/SPIONs to improve tumor targeting efficiencies in MRI scans of FR-positive tumor cells. TEM images revealed that SPIONs were encapsulated by FAPLCS and that FAPLCS/SPIONs, PLCS/SPIONs, FAPLCS, and PLCS micelles are spherical and uniformly shaped. Physical characterization of micelles showed that they had good size distribution, small size, excellent stability, proper magnetic properties, and enhanced MRI sensitivities. Cellular toxicity tests indicated that FAPLCS/SPION micelles possessed low cytotoxicity and excellent biocompatibility. The results of both in vitro and in vivo studies demonstrated that FAPLCS/SPION micelles specifically bound to FR-positive HeLa cells and predominantly accumulated in established HeLa-derived tumors in mice. Signal intensities of T_2-weighted images in established HeLa tumors were reduced dramatically 1 hour after intravenous administration of FAPLCS/SPION micelles. We believe that FAPLCS/SPION micelles have considerable potential for use as safe and effective MRI contrast agents and drug delivery vehicles for the diagnosis and treatment of tumors overexpressing FRs.

Acknowledgments

Disclosure

The authors report no conflicts of interest in this work.

References

1. Nasongkla N, Bey E, Ren J, et al. Multifunctional polymeric micelles as cancer-targeted, MRI-ultrasensitive drug delivery systems. *Nano Lett.* 2006;6(11):2427–2430.
2. Yoo MK, Park IK, Lim HT, et al. Folate-PEG-superparamagnetic iron oxide nanoparticles for lung cancer imaging. *Acta Biomater.* 2012;8(8):3005–3013.
3. Yang X, Grailer JJ, Rowland IJ, et al. Multifunctional SPIO/DOX-loaded wormlike polymer vesicles for cancer therapy and MR imaging. *Biomaterials.* 2010;31(34):9065–9073.
4. Yang HM, Park CW, Woo MA, et al. HER2/neu antibody conjugated poly(amino acid)-coated iron oxide nanoparticles for breast cancer MR imaging. *Biomacromolecules.* 2010;11(11):2866–2872.
5. Lee Y, Lee H, Kim YB, et al. Bioinspired surface immobilization of hyaluronic acid on monodisperse magnetite nanocrystals for targeted cancer imaging. *Adv Mater.* 2008;20(21):4154–4157.
6. Xie J, Chen K, Lee HY, et al. Ultrasmall c(RGDyK)-coated Fe_3O_4 nanoparticles and their specific targeting to integrin alpha(v)beta3-rich tumor cells. *J Am Chem Soc.* 2008;130(24):7542–7543.
7. Crayton SH, Tsourkas A. PH-titratable superparamagnetic iron oxide for improved nanoparticle accumulation in acidic tumor microenvironments. *ACS Nano.* 2011;5(12):9592–9601.
8. Yang X, Chen Y, Yuan R, et al. Folate-encoded and Fe_3O_4-loaded polymeric micelles for dual targeting of cancer cells. *Polymer.* 2008;49(16):3477–3485.
9. Veiseh O, Gunn JW, Zhang M. Design and fabrication of magnetic nanoparticles for targeted drug delivery and imaging. *Adv Drug Deliv Rev.* 2010;62(3):284–304.
10. Harris JM, Chess RB. Effect of pegylation on pharmaceuticals. *Nat Rev Drug Discov.* 2003;2(3):214–221.
11. Kircheis R, Wightman L, Wagner E. Design and gene delivery activity of modified polyethylenimines. *Adv Drug Deliv Rev.* 2001;53(3):341–358.
12. Petri-Fink A, Steitz B, Finka A, Salaklang J, Hofmann H. Effect of cell media on polymer coated superparamagnetic iron oxide nanoparticles (SPIONs): colloidal stability, cytotoxicity, and cellular uptake studies. *Eur J Pharm Biopharm.* 2008;68(1):129–137.
13. Bhattacharya D, Das M, Mishra D, et al. Folate receptor targeted, carboxymethyl chitosan functionalized iron oxide nanoparticles: a novel ultradispersed nanoconjugates for bimodal imaging. *Nanoscale.* 2011;3(4):1653–1662.
14. Zhang J, Rana S, Srivastava RS, Misra RD. On the chemical synthesis and drug delivery response of folate receptor-activated, polyethylene glycol-functionalized magnetite nanoparticles. *Acta Biomater.* 2008;4(1):40–48.
15. Jiang GB, Quan D, Liao K, Wang H. Novel polymer micelles prepared from chitosan grafted hydrophobic palmitoyl groups for drug delivery. *Mol Pharm.* 2006;3(2):152–160.
16. Lin ZT, Song K, Bin JP, Liao YL, Jiang GB. Characterization of polymer micelles with hemocompatibility based on N-succinyl-chitosan grafting with long chain hydrophobic groups and loading aspirin. *J Mater Chem.* 2011;21(47):19153–19165.
17. Martin L, Wilson CG, Koosha F, et al. The release of model macromolecules may be controlled by the hydrophobicity of palmitoyl glycol chitosan hydrogels. *J Control Release.* 2002;80(1–3):87–100.
18. Agrawal P, Strijkers GJ, Nicolay K. Chitosan-based systems for molecular imaging. *Adv Drug Deliv Rev.* 2010;62(1):42–58.
19. Lee CM, Jeong HJ, Kim SL, et al. SPION-loaded chitosan-linoleic acid nanoparticles to target hepatocytes. *Int J Pharm.* 2009;371(1–2):163–169.
20. Yinsong W, Lingrong L, Jian W, Zhang Q. Preparation and characterization of self-aggregated nanoparticles of cholesterol-modified O-carboxymethyl chitosan conjugates. *Carbohydr Polym.* 2007;69(3):597–606.
21. Shi Z, Neoh KG, Kang ET, et al. (Carboxymethyl)chitosan-modified superparamagnetic iron oxide nanoparticles for magnetic resonance imaging of stem cells. *ACS Appl Mater Interfaces.* 2009;1(2):328–335.
22. Hyung Park J, Kwon S, Lee M, et al. Self-assembled nanoparticles based on glycol chitosan bearing hydrophobic moieties as carriers for doxorubicin: in vivo biodistribution and anti-tumor activity. *Biomaterials.* 2006;27(1):119–126.
23. You J, Li X, de Cui F, Du YZ, Yuan H, Hu FQ. Folate-conjugated polymer micelles for active targeting to cancer cells: preparation, in vitro evaluation of targeting ability and cytotoxicity. *Nanotechnology.* 2008;19(4):045102.
24. Liu TY, Chen SY, Lin YL, Liu DM. Synthesis and characterization of amphiphatic carboxymethyl-hexanoyl chitosan hydrogel: water-retention ability and drug encapsulation. *Langmuir.* 2006;22(23):9740–9745.
25. National Research Council of the National Acadamies. *Guide for the Care and Use of Laboratory Animals. 8th ed.* Washington, DC: The National Acadamies Press; 2011. Available from: http://grants.nih.gov/grants/olaw/Guide-for-the-care-and-use-of-laboratory-animals.pdf. Accessed June 1, 2011.
26. Hobbs SK, Monsky WL, Yuan F, et al. Regulation of transport pathways in tumor vessels: role of tumor type and microenvironment. *Proc Natl Acad Sciences U S A.* 1998;95(8):4607–4612.
27. Rieder H, Meyer zum Büschenfelde KH, Ramadori G. Functional spectrum of sinusoidal endothelial liver cells. Filtration, endocytosis, synthetic capacities and intercellular communication. *J Hepatol.* 1992;15(1–2):237–250.
28. Owens DE 3rd, Peppas NA. Opsonization, biodistribution, and pharmacokinetics of polymeric nanoparticles. *Int J Pharm.* 2006;307(1):93–102.
29. Minchin RF, Martin DJ. Nanoparticles for molecular imaging – an overview. *Endocrinology.* 2010;151(2):474–481.
30. Li T, Longobardi L, Granero-Molto F, Myers TJ, Yan Y, Spagnoli A. Use of glycol chitosan modified by 5beta-cholanic acid nanoparticles for the sustained release of proteins during murine embryonic limb skeletogenesis. *J Control Release.* 2010;144(1):101–108.
31. Gupta AK, Gupta M. Synthesis and surface engineering of iron oxide nanoparticles for biomedical applications. *Biomaterials.* 2005;26(18):3995–4021.
32. Lu J, Ma S, Sun J, et al. Manganese ferrite nanoparticle micellar nanocomposites as MRI contrast agent for liver imaging. *Biomaterials.* 2009;30(15):2919–2928.
33. Fan C, Gao W, Chen Z, et al. Tumor selectivity of stealth multi-functionalized superparamagnetic iron oxide nanoparticles. *Int J Pharm.* 2011;404(1–2):180–190.
34. Lee PW, Hsu SH, Wang JJ, et al. The characteristics, biodistribution, magnetic resonance imaging and biodegradability of superparamagnetic core-shell nanoparticles. *Biomaterials.* 2010;31(6):1316–1324.
35. Wang YX. Superparamagnetic iron oxide based MRI contrast agents: Current status of clinical application. *Quant Imaging Med Surg.* 2011;1(1):35–40.
36. Bagnoli M, Tomassetti A, Figini M, et al. Downmodulation of caveolin-1 expression in human ovarian carcinoma is directly related to alpha-folate receptor overexpression. *Oncogene.* 2000;19(41):4754–4763.
37. Thorek DL, Chen AK, Czupryna J, Tsourkas A. Superparamagnetic iron oxide nanoparticle probes for molecular imaging. *Ann Biomed Eng.* 2006;34(1):23–38.
38. Sun C, Lee JS, Zhang M. Magnetic nanoparticles in MR imaging and drug delivery. *Adv Drug Deliv Rev.* 2008;60(11):1252–1265.
39. Chen TJ, Cheng TH, Hung YC, Lin KT, Liu GC, Wang YM. Targeted folic acid-PEG nanoparticles for noninvasive imaging of folate receptor by MRI. *J Biomed Mater Res A.* 2008;87(1):165–175.

Supplementary material
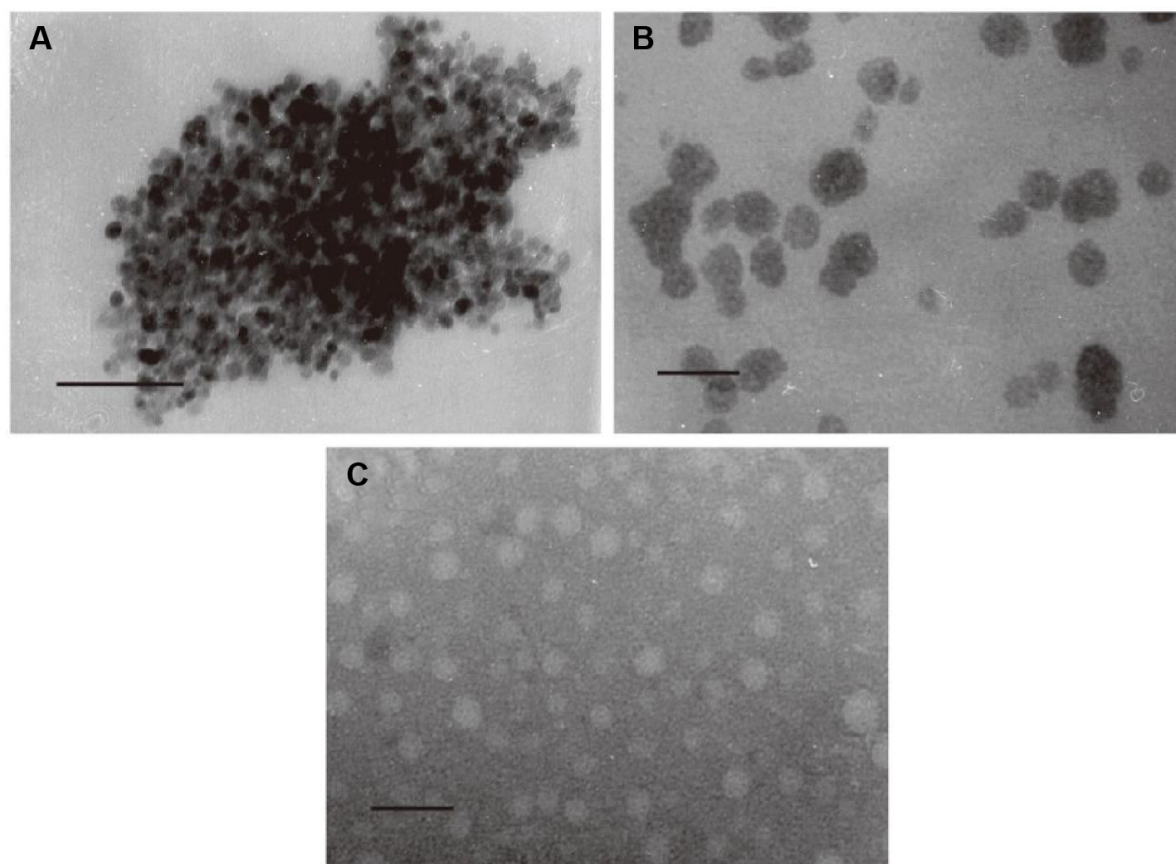
Figure S1 TEM images of bare SPIONs, PLCS/SPION micelles, and PLCS micelles.
Notes: TEM images of bare SPIONs (**A**), PLCS/SPION micelles (**B**), and PLCS micelles (**C**).
Abbreviations: TEM, transmission electron microscopy; PLCS, N-palmitoyl chitosan; SPION, superparamagnetic iron oxide nanoparticle.